Implementation and Performance Evaluation of a Broad-Band Power Spectrum Analyzer

Gaetano Pasini, *Member, IEEE*, Domenico Mirri, *Member, IEEE*, Gaetano Iuculano, and Fabio Filicori, *Member, IEEE*

***Abstract*—A new technique for power spectrum analysis is introduced, theoretically evaluated, and experimentally verified with a prototype. This technique is based on the estimate of the autocorrelation function for different delays. The proposed sampling strategy is random in the time domain and equally spaced, synchronous with the signal, in the delay domain. It is shown that the estimate of the power spectral components is asymptotically unbiased, and the experimental results are also given.**

***Index Terms*—Hardware implementation, performance evaluation, power spectrum instrument, random sampling strategy, wide-band spectrum analysis.**

I. Introduction

A POWER spectrum analyzer whose bandwidth is not limited by the mean sampling time, which depends on the conversion time of the ADC and the aperture time of the S/H, was previously introduced by the authors [1]. The procedure was based on the estimation of the spectral components of the autocorrelation function of the input signal through the simultaneous random sampling of the given input signal and its randomly "delayed copy." The samples were therefore randomly taken in a double-dimension space, time, and delay. By using a random process in the time domain with a recursive technique previously introduced by the authors in order to avoid any bandwidth limitation due to the sampling strategy [2], it was shown that the estimate of the power spectral components is asymptotically unbiased. Now, a similar new technique for power spectrum analysis is introduced in which the samples are taken randomly in the time domain and equally spaced in the delay domain, synchronous with the period of the input signal. This means that the sampling delay with respect to each random sampling instant, which is used for the estimation of the autocorrelation function of the input signal, is uniformly distributed in an interval equal to the period of the input signal. Because this sampling strategy also is random in the time domain, any bandwidth limitation due to the conversion time of the ADC is avoided. In this paper, the theoretical findings and the experimental results on a prototype based on the proposed sampling technique are given.

Manuscript received May 4, 2000; revised June 8, 2001.

G. Pasini and D. Mirri are with the Department of Electrical Engineering, University of Bologna, Bologna, Italy (e-mail: gaetano.pasini@mail.ing.unibo.it).

G. Iuculano is with the Department of Electronics, Engineering Faculty, University of Firenze, Firenze, Italy.

F. Filicori is with the Department of Electronics, Engineering Faculty, University of Bologna, Bologna, Italy.

Publisher Item Identifier S 0018-9456(01)07892-5.

II. Measurement Procedure

Let us consider the Fourier series of a finite spectrum periodic alternated signal $x(t)$ with period $T_1 = 1/f_1$

$$x(t) = \sum_{\substack{n=-M \\ n\neq 0}}^{+M} X_n e^{j2\pi n f_1 t} \tag{1}$$

where n is an integer and the spectral coefficients $X_n = |X_n| e^{j\varphi_n}$ can be derived from

$$X_n = \frac{1}{T_1} \int_{-T_1/2}^{+T_1/2} x(t) e^{-j2\pi n f_1 t}\, dt. \tag{2}$$

When the signal is real, i.e., $x(t) = x^*(t)$, it follows that $X_n^* = X_{-n}$. The autocorrelation function of the real signal $x(t)$ is given by [1]

$$\begin{aligned} r(\tau) &= \frac{1}{T_1} \int_{-T_1/2}^{+T_1/2} x(t)x(t+\tau)\, dt \\ &= \sum_{\substack{n=-M \\ n\neq 0}}^{+M} |X_n|^2 e^{j2\pi n f_1 \tau} \\ &= \sum_{\substack{n=-M \\ n\neq 0}}^{+M} |X_n|^2 \cos(2\pi n f_1 \tau) \end{aligned} \tag{3}$$

and it still contains all the information concerning the signal power spectrum components, i.e., $|X_n|^2$. The frequency allocation of each spectral component of $x(t)$ and $r(\tau)$ is the same; besides the phase angle of each spectral component of $x(t)$ disappears in the evaluation of $r(\tau)$, which therefore results in a real, even function of the delay τ. Because the autocorrelation function is also a discrete spectrum signal with period T_1, we can write [2]

$$\begin{aligned} |X_n|^2 &= \frac{1}{T_1} \int_{-T_1/2}^{+T_1/2} r(\tau) e^{-j2\pi n f_1 \tau}\, d\tau \\ &= \frac{1}{T_1} \int_{-T_1/2}^{+T_1/2} r(\tau) \cos(2\pi n f_1 \tau)\, d\tau. \end{aligned} \tag{4}$$

For the digital implementation of the autocorrelation function, the signal $x(t)$ is sampled in correspondence to a sequence of N successive couples of delayed instants, and the autocorrelation function is estimated with a moving average filter

$$\tilde{r}_{lN}(\tau) = \frac{1}{N} \sum_{i=0}^{N-1} x(t_{lN-i}) x(t_{lN-i} + \tau) \tag{5}$$

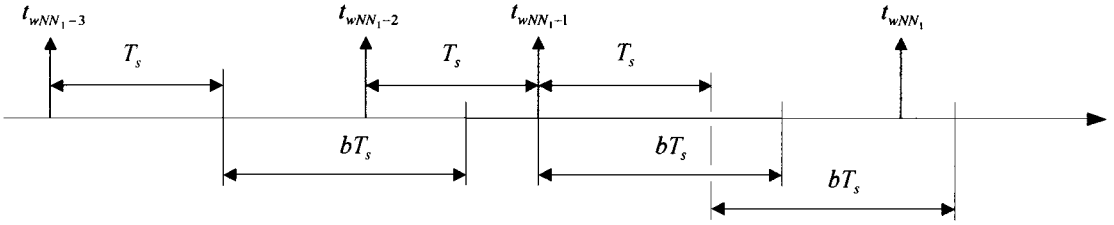

Fig. 1. Sequence of random sampling instants.

where

lN N-multiple integer that marks the generic estimated autocorrelation function,

i generic value of the sequence, and

t_{lN-i} sampling instant.

By using the random sampling strategy described by this additive model, which defines a recursive random process

$$t_{lN-i} = t_{lN-i-1} + (1 + Y_{lN-i})T_s \tag{6}$$

where T_s is a constant and Y_{lN-i} a random variable uniformly distributed in the interval (0, $b \approx 1.5$), it can be shown that the estimate of the autocorrelation function is characterized, independently from the shift value τ, by a bandwidth that is not influenced by the minimum sampling time T_s and limited uniquely by the bandwidth of the S/H circuit adopted [3]. Now, a Discrete Fourier Transform of equally-spaced samples of $\tilde{r}_{lN}(\tau)$ in the τ-space, i.e., $\tau_k = k\Delta\tau$ with k an integer, directly leads to the required harmonics $|X_n|^2$ of the corresponding power spectrum of the signal $x(t)$. By assuming a synchronous sampling strategy, i.e., $\Delta\tau = T_1/N_1$ with $N_1 > 2M$ (in order to avoid aliasing), and marking with the label w a generic output $|\tilde{X}_{n,w}|^2$, i.e., the estimate $|\tilde{X}_{n,w}|^2$ of the nth spectral component of the power spectrum, obtained with a sequence of NN_1 couples of sampling instants, we deduce from (4) and (5) that the result is

$$\begin{aligned}\left|\tilde{X}_{n,w}\right|^2 &= \frac{1}{N_1}\sum_{k=1}^{N_1}\tilde{r}_{wNN_1}\left(k\frac{T_1}{N_1}\right)\cos\left(2\pi\frac{nk}{N_1}\right)\\ &= \frac{1}{N}\frac{1}{N_1}\sum_{k=1}^{N_1}\sum_{i=(k-1)N}^{kN-1} x\left(t_{wNN_1-i}\right)\\ &\quad\cdot x\left(t_{wNN_1-i}+k\frac{T_1}{N_1}\right)\cos\left(2\pi\frac{nk}{N_1}\right).\end{aligned} \tag{7}$$

Therefore, for each of the N_1 delays, a sequence of N random couples of sampling instants is introduced.

III. Criterion for Performance Analysis

By substituting (1) into (7) we can write

$$\begin{aligned}\left|\tilde{X}_{n,w}\right|^2 &= \frac{1}{N}\frac{1}{N_1}\sum_{k=1}^{N_1}\sum_{i=(k-1)N}^{kN-1}\sum_{\substack{q=-M\\ q\neq 0}}^{+M}\sum_{\substack{m=-M\\ m\neq 0}}^{+M} X_q X_m\\ &\quad\cdot e^{j2\pi(q+m)f_1 t_{wNN_1-i}} e^{j2\pi m(k/N_1)}\cos\left(2\pi\frac{nk}{N_1}\right).\end{aligned} \tag{8}$$

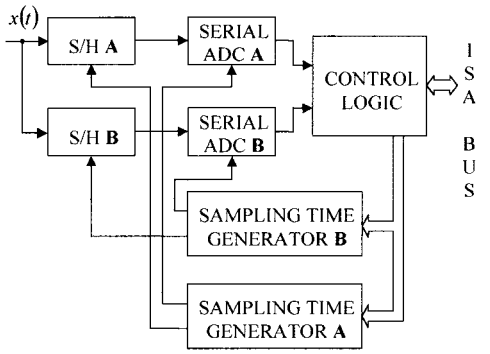

Fig. 2. Block diagram of the instrument.

The global contribution in (8) of the terms with $q + m = 0$ coincides with the estimated parameter $|X_n|^2$ given by (4). In fact, for $q + m = 0$ we obtain

$$\begin{aligned}\left|\tilde{X}_{n,w}\right|^2_{q+m=0} &= \frac{1}{N_1}\sum_{\substack{q=-M\\ q\neq 0}}^{+M}|X_q|^2\sum_{k=1}^{N_1}\cos\left(2\pi\frac{nk}{N_1}\right)\\ &\quad\cdot e^{-j2\pi q(k/N_1)}.\end{aligned} \tag{9}$$

On the other hand, we have

$$\begin{aligned}&\sum_{k=1}^{N_1}\cos\left(2\pi\frac{nk}{N_1}\right)e^{-j2\pi q(k/N_1)}\\ &\quad=\sum_{k=1}^{N_1}\tfrac{1}{2}\left(e^{-j2\pi(q-n)(k/N_1)}+e^{-j2\pi(q+n)(k/N_1)}\right)\\ &\quad=\begin{cases}\dfrac{N_1}{2} & \text{for } q=\pm n\\ 0 & \text{elsewhere}\end{cases}\end{aligned} \tag{10}$$

due to the well known property of geometric progressions

$$\begin{aligned}\sum_{k=1}^{N_1}e^{-j2\pi k(q\pm n/N_1)} &= e^{-j2\pi(q\pm n/N_1)}\frac{e^{-j2\pi(q\pm n)}-1}{e^{-j2\pi(q\pm n/N_1)}-1}\\ &=\begin{cases}N_1 & \text{for } q\pm n=0\\ 0 & \text{elsewhere.}\end{cases}\end{aligned} \tag{11}$$

As a consequence of (10), the sum with respect to q in (9) has only two terms, when $q \pm n = 0$. Therefore, we verify that

$$\left|\tilde{X}_{n,w}\right|^2_{q+m=0} = |X_n|^2 \tag{12}$$

and (8) can be expressed as follows

$$\left|\tilde{X}_{n,w}\right|^2 = |X_n|^2 + \Delta_{n,w} \tag{13}$$

where

$$\Delta_{n,w} = \frac{1}{NN_1} \sum_{k=1}^{N_1} \sum_{i=(k-1)N}^{kN-1} \sum_{\substack{q=-M \\ q\neq 0 \\ q+m\neq 0}}^{+M} \sum_{\substack{m=-M \\ m\neq 0}}^{+M} X_q X_m \cdot e^{j2\pi(q+m)f_1 t_{wNN_1-i}} \cos\left(2\pi \frac{nk}{N_1}\right) e^{j2\pi m(k/N_1)}. \quad (14)$$

The initial one of the NN_1 couples of sampling instants used to generate the first value of the output sequence labeled with w is given by

$$t_{(w-1)NN_1+1} = t_I + \left(1 + Y_{(w-1)NN_1+1}\right) T_s \quad (15)$$

where t_I is the unknown shift between the initial sampling instant and the time origin of $x(t)$. Any actual value of t_I can be assumed as a representation of a continuous random variable uniformly distributed in some generic time interval $(-T/2, +T/2, T$ being unknown) [4]. Beginning at the first instant and applying (9) recursively, we obtain

$$t_{wNN_1-i} = t_I + \left[NN_1 - i + \sum_{r=(w-1)NN_1+1}^{wNN_1-i} Y_r \right] T_s. \quad (16)$$

The random variables $\{Y_r\}$ are mutually independent and do not depend on t_I. By substituting (16) into (14), after simple manipulations, we can write

$$\Delta_{n,w} = \frac{1}{NN_1} \sum_{\substack{q=-M \\ q\neq 0}}^{+M} \sum_{\substack{m=-M \\ m\neq 0}}^{+M} X_q X_m e^{j2\pi(q+m)f_1 t_I} \cdot e^{j2\pi(q+m)NN_1 f_1 T_s} \sum_{k=1}^{N_1} \cos\left(2\pi \frac{nk}{N_1}\right) \cdot e^{j2\pi m(k/N_1)} \sum_{i=(k-1)N}^{kN-1} e^{-j2\pi(q+m)if_1 T_s} \cdot \exp\left(j2\pi(q+m)f_1 T_s \sum_{r=(w-1)NN_1+1}^{wNN_1-i} Y_r \right) \quad (17)$$

which is the random error introduced by the estimate. An appropriate characterization of the output uncertainty can be obtained by evaluating the statistical parameters of the output $|\tilde{X}_{n,w}|^2$, i.e., the mean value $E\{|\tilde{X}_{n,w}|^2\}$ and the mean squared error $E\{(|\tilde{X}_{n,w}|^2 - |X_n|^2)^2\}$. In order to avoid the influence of the conventional time origin on the instrument performance, the excursion of the initial shift t_I, i.e., T, must be sufficiently large and theoretically must tend to infinity. Therefore, we have the asymptotic mean

$$\lim_{T\to\infty} E\left\{ \left| \tilde{X}_{n,w} \right|^2 \right\}. \quad (18)$$

In the following, only the errors arising from the sampling strategy and the filtering procedures are considered since this paper aims to deduce the specific properties of the proposed sampling strategy and to compare it with the other one. It can be shown (see the Appendix) that the output of the instrument is asymptotically unbiased, i.e.,

$$\lim_{T\to\infty} E\left\{ \left| \tilde{X}_{n,w} \right|^2 \right\} = |X_n|^2. \quad (19)$$

IV. Hardware Implementation

The measurement procedure previously described requires the acquisition of two pulse sequences of the signal, based on the random strategy of (6) and delayed by the quantity $\tau_k = k\Delta\tau$. An example of the random pulse sequence is described in Fig. 1. From this figure, we deduce that, as provided from (6), the minimum time interval between two successive sampling instants is equal to T_s. The minimum value of T_s is equal to the time required by the acquisition system to complete a conversion cycle and to be available for a new sampling command.

Fig. 2 shows the block diagram of the realized instrument. The two generators are synchronized so that channel A samples the input signal in the instant t_{wNN_1-i} and the channel B in the instant $t_{wNN_1-i} + \tau_k$. The instrument was implemented in a single board with an ISA (Industry Standard Architecture) compatible bus connector.

In order to reduce the instrument complexity, ADCs having a serial output were used. In fact, by using an ADC with parallel output, we must put a 16-bit wide internal bus on the realized board in order to connect each ADC to the control logic and then to the ISA bus. Instead, a serial ADC allows a reduction of the board complexity: each ADC is directly connected to the control logic section by means of a serial link. The conversion of data representation (from serial to parallel, 16-bits wide) was made inside the control logic, and successive data are transferred to the ISA bus. The conversion from serial to parallel is quite complex, but it is all implemented inside a single field programmable gate array (FPGA) chip for both of the ADCs, so that the 16-bit wide bus is extended only from the FPGA to the ISA connector. Inside this last device was also implemented the control logic used to generate all the auxiliary signals required for the correct operation of the board.

The identical sampling time generators generate completely programmable sampling signals, i.e., it is possible to define the time interval between each rising edge of the delayed pulses with a theoretical resolution of about 50 ps. This value practically rises to 200 ps due to the noise time jitter. In addition, the time interval between the successive sampling pulses of each sequence can be varied between 2 μs and 1 ms. Due to the total programmability of this time interval generator, it is possible to generate a lot of different sampling strategies (for instance, random recursive or not, synchronous or not, etc.). The small resolution of this generator is a very important parameter, because this quantity, together with the bandwidth of the S/H devices, will bound the maximum frequency of this power spectrum analyzer.

The sampling time generator can be logically split into two parts: a counter and a variable phase sinusoidal signal generator, driven by the same clock generator of frequency f_c and connected as shown in Fig. 3. An external processor sends through

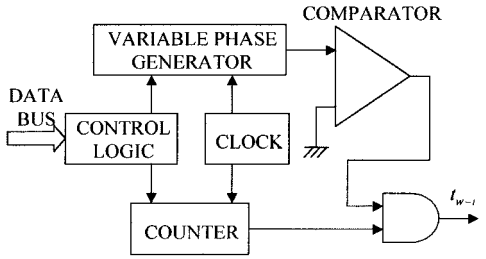

Fig. 3. Block diagram of the sampling time generator.

the data bus a numerical quantity that defines the time interval to be generated. This quantity is split (with a proper software subroutine through the control logic block) into two numbers: the first applied to the counter, and the second one applied to the variable phase generator. The counter starts from the programmed state and makes a countdown until it reaches zero. The logical transition when the counter recycles to zero is applied to an AND gate. The numerical data applied to the phase generator (based on the digital direct synthesis) defines the phase of a sinusoidal signal (of frequency $f_c/4$) and constant amplitude, which is applied to the input of a comparator, referred to the zero level. The comparator output is applied to the other input of the AND gate. Therefore, the time interval depends on two quantities: the first is the time necessary for the down counter to reach the zero level and the second one is the time from this instant to the one when the variable phase signal crosses zero level with a rising edge. In this way, the counter defines the largest part of the time interval amplitude and the variable phase generator allows increasing the resolution.

The sample-and-hold circuits are the SHC605 from Burr–Brown. Their characteristics are as follows: full power bandwidth 32 MHz, dynamic range of 77 dB at 5 MHz and 20 MS/s sampling rate, acquisition time 60 ns, slew rate 200 V/μs, and maximum droop rate 8 mV/μs. The analog-to-digital converter is the ADS7809 also from Burr–Brown. It is a 16-bit sampling ADC with a conversion time of 10 μs, integral nonlinearity of 2 LSBs, no missing codes, and full power bandwidth of 250 kHz. A sampling ADC was used to reduce effects of the S/H droop rate. In fact, with a conversion time of 10 μs, the effect of S/H droop rate is about 80 mV, more than 10^3 LSBs.

V. Experimental Results

In order to show that with the proposed method the minimum sampling interval T_s does not limit the instrument bandwidth, a relatively large value of $T_s = 150$ μs in (6) was chosen. In a conventional digital instrument implementation, based on an equally-spaced sampling strategy, the instrument bandwidth would have been limited to $f_{\max} = (1/300)10^6 \cong 3.3$ kHz, according to the sampling theorem. Instead, since the resolution in the time delay generation can easily be much greater (200 ps in our case), the corresponding bandwidth limitation becomes $f_{\max} = (1/400)10^{12} = 2.5 \cdot 10^3$ MHz. Thus, in our case, the instrument bandwidth is practically limited by the bandwidth of the adopted S/Hs, which is equal to 32 MHz.

Table I shows the power spectrum components of a sinusoidal signal at the frequency $f_1 = 1$ MHz, evaluated by estimating the autocorrelation function of the signal with a sequence of $N = 32$ sampling instants, and by considering $N_1 = 64$ equally-spaced delayed sequences, synchronous with the input signal. The values of the input signal were measured with the spectrum analyzer HP8590L and the multimeter HP3458A, used as references in order to deduce the absolute error. The relative error in the measurement of the sinusoidal signal is 1%, showing a good approximation to the experimental result.

TABLE I
Power Spectrum Components of a Sinusoidal Signal at $f_1 = 1$ MHz

Harmonic order	Power spectrum (V^2)	Absolute error (V^2)
0	0.0043	0.0020
1	0.247	0.002
2	0.0024	0.0024
3	0.0019	0.0019
4	0.0023	0.0023
5	0.00096	0.00096
6	0.0043	0.0043
7	0.00051	0.00051
8	0.00035	0.00035
9	0.0012	0.0012
10	0.0011	0.0011

In Table II, the fundamental power spectrum of different sinusoidal signals between $f_1 = 10$ Hz, $f_1 = 30$ MHz and the relative error are given. The selected values of N and N_1 are also reported. It is interesting to observe that the minimum sampling time between two successive sampling instants of each sequence is $T_s = 150$ μs, confirming that the mean sampling time does not limit the bandwidth of the instrument. Besides, the bandwidth limitation due to the S/Hs becomes relevant when $f_1 \geq 5$ MHz.

Table III shows the first ten power spectrum components of a square wave signal with $f_1 = 0.5$ MHz, $N = 8$, and $N_1 = 256$. It is interesting to observe that the odd harmonic components of the signal are measured with a good approximation and that the even harmonic components of the signal are negligible by assuming a resolution of the order of some $(\text{mV})^2$.

The experimental results were in good agreement with the theoretical findings, showing that the estimate of the power spectral components is asymptotically unbiased on the hypothesis of a synchronized random sampling in the delay domain, and that the bandwidth of the instrument is limited uniquely either by the bandwidth of the S/H circuits or the resolution in the delay domain. The bandwidth of the S/H circuits is much less than the bandwidth limitation due to the sampling theorem applied to the delay domain, where a synchronous equally spaced sampling strategy is used; these values were selected only for convenience because the main proposal of the paper is to show that the sampling strategy in the time domain does not limit the bandwidth of the instrument when a convenient random sampling strategy is used. In this hypothesis, the A/D conversion time does not influence the bandwidth of the instrument.

TABLE II
FUNDAMENTAL POWER SPECTRUM OF DIFFERENT SINUSOIDAL SIGNALS

Frequency (kHz)	Power spectrum (V^2)	Relative error (%)	N	N_1
0.01	0.249	0.4	16	128
0.05	0.248	0.4	16	128
0.1	0.248	0.8	16	128
0.5	0.249	0.1	32	64
1	0.250	-0.1	32	64
10	0.245	-0.04	32	64
50	0.245	1.6	32	64
100	0.247	1.2	32	64
200	0.242	0.3	32	64
500	0.245	1.6	32	64
1000	0.247	1.2	32	64
2000	0.248	0.4	16	128
5000	0.243	2.6	16	128
10000	0.237	5.1	16	128
15000	0.223	10	8	256
20000	0.209	16	16	128
30000	0.171	31	8	256

TABLE III
FIRST TEN COMPONENTS OF A SQUARE WAVE SIGNAL WITH $f_1 = 0.5$ MHz

Harmonic order	Power spectrum (V^2)	Absolute error (V^2)
0	0.00085	0.00085
1	0.41	0.05
2	0.0011	0.0011
3	0.045	0
4	0.0022	0.0022
5	0.016	0
6	0.0013	0.0013
7	0.0066	0.0015
8	0.0021	0.0021
9	0.0022	0.0027
10	0.0035	0.0035

VI. CONCLUSIONS

A new procedure for the evaluation of the power spectral components of a periodic signal is proposed, and the experimental results on a prototype are given. This procedure is based on the estimate in the time domain of the autocorrelation function by using a convenient random sampling strategy (which does not introduce any bandwidth limitation), and on the estimate of each spectral component of the signal by using time delayed sequences, synchronous with the input signal. The differential nature of the delay enables an accurate delay control for a given hardware since any "common mode" source of timing errors (i.e., phase noise in the clock oscillator or any other "common-mode" noise/interference source) is intrinsically compensated. Therefore, this method allows overcoming the bandwidth limitation inherent to the time domain equally-spaced spectral analysis. The bandwidth limitation, imposed by the sampling theorem, is transferred from the time domain to the delay domain, where the variability in the delay can be finely controlled because it is influenced essentially by the time-jitter. The experimental results with a prototype were in very good agreement with the theoretical findings.

APPENDIX

For the evaluation of the statistical parameters of the estimator $|\tilde{X}_{n,w}|^2$ of a generic squared spectral component $|X_n|^2$ of the input signal $x(t)$, it is convenient to rewrite (17) as follows

$$\Delta_{n,w} = \sum_{\substack{q=-M \\ q\neq 0 \\ q+m\neq 0}}^{+M} \sum_{\substack{m=-M \\ m\neq 0}}^{+M} X_q X_m e^{j2\pi(q+m)f_1 t_I} F_{q,m}(\underline{Y}) \quad \text{(A1)}$$

where $\underline{Y}$ is a congruent vector of the random variables $\{Y_r\}$ and we have assumed

$$F_{q,m}(\underline{Y}) = \frac{1}{NN_1} e^{j2\pi(q+m)f_1 T_s} \sum_{k=1}^{N_1} \cos\left(2\pi \frac{nk}{N_1}\right) \cdot e^{j2\pi m(k/N_1)} \sum_{i=(k-1)N}^{kN-1} e^{-j2\pi(q+m)if_1 T_s} \cdot \exp\left(j2\pi(q+m)f_1 T_s \sum_{r=(w-1)NN_1+1}^{wNN_1-i}\right) Y_r. \quad \text{(A2)}$$

The random function $F_{q,m}(\underline{Y})$ is independent of t_I.

From (13) the expected value of the estimate $|\tilde{X}_{n,w}|^2$ is

$$E\left\{\left|\tilde{X}_{n,w}\right|^2\right\} = |X_n|^2 + E\{\Delta_{n,w}\}. \quad \text{(A3)}$$

On the other hand, from (A1) we deduce

$$E\{\Delta_{n,w}\} = \sum_{\substack{q=-M \\ q\neq 0 \\ q+m\neq 0}}^{+M} \sum_{\substack{m=-M \\ m\neq 0}}^{+M} X_q X_m E\left\{e^{j2\pi(q+m)f_1 t_I}\right\} E\{F_{q,m}(\underline{Y})\}. \quad \text{(A4)}$$

The continuous random variable t_I, uniformly distributed in the interval $\pm T/2$, has the following characteristic function

$$E\left\{e^{j2\pi\alpha t_I}\right\} = \int_{-T/2}^{+T/2} f(t) e^{j2\pi\alpha t}\, dt = \frac{1}{T} \frac{e^{j\pi\alpha T} - e^{-j\pi\alpha T}}{j2\pi\alpha} = \frac{\sin(\pi\alpha T)}{\pi\alpha T} = \operatorname{sinc}(\alpha T) \quad \text{(A5)}$$

where $f(t) = 1/T$ is the uniform probability density. The limiting value of (A5) for T tending to infinity and $\alpha = (q+m)f_1$ is

$$\lim_{T\to\infty} E\left\{e^{j(q+m)\omega_1 t_I}\right\} = \begin{cases} 1 & \text{for } q+m=0 \\ 0 & \text{elsewhere.} \end{cases} \tag{A6}$$

Since in the double sum of (A4) the quantity $q+m$ must be always different than zero, it follows that

$$\lim_{T\to\infty} E\left\{\Delta^2_{n,w}\right\} = 0 \tag{A7}$$

and, consequently, the asymptotic mean of $|\tilde{X}_{n,w}|^2$ becomes

$$\lim_{T\to\infty} E\left\{\left|\tilde{X}_{n,w}\right|^2\right\} = |X_n|^2. \tag{A8}$$

The asymptotic bias is therefore null.

REFERENCES

[1] D. Mirri, G. Iuculano, G. Pasini, F. Filicori, and L. Peretto, "A broad-band power spectrum analyzer based on twin-channel delayed sampling," *IEEE Trans. Instrum. Meas.*, vol. 47, pp. 1346–1354, Oct. 1998.

[2] D. Mirri, G. Iuculano, A. Menchetti, F. Filicori, and M. Catelani, "Recursive random sampling strategy for a digital wattmeter," in *IEEE Instrum. Meas. Technol. Conf.*, New York, May 1992, pp. 577–582.

[3] W. McC. Siebert, *Circuits, Signals, and Systems*. New York: McGraw-Hill, 1986.

[4] W. Feller, *An Introduction to Probability Theory and Its Applications*. New York: Wiley, 1971.

Gaetano Pasini (M'97) was born in Italy in 1964. He received the degree in electronic engineering from the University of Bologna, Bologna, Italy.

He is currently a Researcher in electrical measurement, University of Bologna. His research activity is mainly oriented to digital signal processing in electronic instruments, power measurements, and characterization of nonlinear systems with memory.

Domenico Mirri (M'91) was born in Italy in 1936. He received the electronic engineering degree from the University of Bologna, Bologna, Italy.

Presently, he is a Full Professor of electronic measurement at the University of Bologna. His current research interest is in the areas of digital measurement instruments, devices metrological characterization, and biomedical measurements.

Gaetano Iuculano was born in Italy in 1938. He received the degree in electronic engineering from the University of Bologna, Bologna, Italy.

Presently he is a Full Professor of electrical measurements at the University of Florence, Florence, Italy. His current research are in calibration applications, reliability analysis and life testing for electronic devices and systems, statistical analysis, and digital measurement instruments.

Fabio Filicori (M'98) was born in Italy in 1949. He received the degree in electronic engineering from the University of Bologna, Bologna, Italy, in 1964.

Presently, he is a Full Professor of applied electronics at the University of Bologna. His current research interests are in the areas of nonlinear circuit analysis and design, electronic devices modeling, digital measurement instruments, and power electronics.